

Lecture Notes in Networks and Systems 944


Duy Cuong Nguyen · Do Trung Hai ·
Ngoc Pi Vu · Banh Tien Long ·
Horst Puta · Kai-Uwe Sattler *Editors*

Advances in Engineering Research and Application

Proceedings of the International
Conference on Engineering Research and
Applications, ICERA 2023, Volume 2

 Springer

Series Editor

Janusz Kacprzyk , *Systems Research Institute, Polish Academy of Sciences, Warsaw, Poland*

Advisory Editors

Fernando Gomide, *Department of Computer Engineering and Automation—DCA, School of Electrical and Computer Engineering—FEEC, University of Campinas—UNICAMP, São Paulo, Brazil*

Okyay Kaynak, *Department of Electrical and Electronic Engineering, Bogazici University, Istanbul, Türkiye*

Derong Liu, *Department of Electrical and Computer Engineering, University of Illinois at Chicago, Chicago, USA*

Institute of Automation, Chinese Academy of Sciences, Beijing, China

Witold Pedrycz, *Department of Electrical and Computer Engineering, University of Alberta, Alberta, Canada*

Systems Research Institute, Polish Academy of Sciences, Warsaw, Poland

Marios M. Polycarpou, *Department of Electrical and Computer Engineering, KIOS Research Center for Intelligent Systems and Networks, University of Cyprus, Nicosia, Cyprus*

Imre J. Rudas, *Óbuda University, Budapest, Hungary*

Jun Wang, *Department of Computer Science, City University of Hong Kong, Kowloon, Hong Kong*

The series “Lecture Notes in Networks and Systems” publishes the latest developments in Networks and Systems—quickly, informally and with high quality. Original research reported in proceedings and post-proceedings represents the core of LNNS.

Volumes published in LNNS embrace all aspects and subfields of, as well as new challenges in, Networks and Systems.

The series contains proceedings and edited volumes in systems and networks, spanning the areas of Cyber-Physical Systems, Autonomous Systems, Sensor Networks, Control Systems, Energy Systems, Automotive Systems, Biological Systems, Vehicular Networking and Connected Vehicles, Aerospace Systems, Automation, Manufacturing, Smart Grids, Nonlinear Systems, Power Systems, Robotics, Social Systems, Economic Systems and other. Of particular value to both the contributors and the readership are the short publication timeframe and the worldwide distribution and exposure which enable both a wide and rapid dissemination of research output.

The series covers the theory, applications, and perspectives on the state of the art and future developments relevant to systems and networks, decision making, control, complex processes and related areas, as embedded in the fields of interdisciplinary and applied sciences, engineering, computer science, physics, economics, social, and life sciences, as well as the paradigms and methodologies behind them.

Indexed by SCOPUS, EI Compendex, INSPEC, WTI Frankfurt eG, zbMATH, SCImago.

All books published in the series are submitted for consideration in Web of Science.

For proposals from Asia please contact Aninda Bose (aninda.bose@springer.com).

Duy Cuong Nguyen · Do Trung Hai ·
Ngoc Pi Vu · Banh Tien Long · Horst Puta ·
Kai-Uwe Sattler
Editors

Advances in Engineering Research and Application

Proceedings of the International Conference
on Engineering Research and Applications,
ICERA 2023, Volume 2

Editors

Duy Cuong Nguyen
Faculty of Electronic Engineering
Thai Nguyen University of Technology
Thai Nguyen, Vietnam

Do Trung Hai
Faculty of Electronic Engineering
Thai Nguyen University of Technology
Thai Nguyen, Vietnam

Ngoc Pi Vu
Faculty of Mechanical Engineering
Thai Nguyen University of Technology
Thai Nguyen, Vietnam

Banh Tien Long
Vietnam Association for Science Editing
Hanoi University of Science and Technology
Hanoi, Vietnam

Horst Puta
Institute for Automation and Systems
Engineering
Ilmenau University of Technology (IUT)
Ilmenau, Germany

Kai-Uwe Sattler
Ilmenau University of Technology (IUT)
Ilmenau, Germany

ISSN 2367-3370

ISSN 2367-3389 (electronic)

Lecture Notes in Networks and Systems

ISBN 978-3-031-62234-2

ISBN 978-3-031-62235-9 (eBook)

<https://doi.org/10.1007/978-3-031-62235-9>

© The Editor(s) (if applicable) and The Author(s), under exclusive license
to Springer Nature Switzerland AG 2024

This work is subject to copyright. All rights are solely and exclusively licensed by the Publisher, whether the whole or part of the material is concerned, specifically the rights of translation, reprinting, reuse of illustrations, recitation, broadcasting, reproduction on microfilms or in any other physical way, and transmission or information storage and retrieval, electronic adaptation, computer software, or by similar or dissimilar methodology now known or hereafter developed.

The use of general descriptive names, registered names, trademarks, service marks, etc. in this publication does not imply, even in the absence of a specific statement, that such names are exempt from the relevant protective laws and regulations and therefore free for general use.

The publisher, the authors and the editors are safe to assume that the advice and information in this book are believed to be true and accurate at the date of publication. Neither the publisher nor the authors or the editors give a warranty, expressed or implied, with respect to the material contained herein or for any errors or omissions that may have been made. The publisher remains neutral with regard to jurisdictional claims in published maps and institutional affiliations.

This Springer imprint is published by the registered company Springer Nature Switzerland AG
The registered company address is: Gewerbestrasse 11, 6330 Cham, Switzerland

If disposing of this product, please recycle the paper.

Preface

This book covers the proceedings of the 6th International Conference on Engineering Research and Application 2023 (ICERA 2023) that was organized by Thai Nguyen University of Technology (TNUT), Vietnam, and cooperated with Ilmenau University of Technology, Germany. In 2018, the first conference was held. Thus far, the conference has attracted a lot of contributions from researchers of many different universities around the world.

This conference aims to bring together researchers from many fields related to engineering research and applications, theories, and practices. This volume covers the following subjects: Mechanical Engineering, Materials and Mechanics of Materials, Mechatronics and Micromechatronics, Automotive Engineering, Electrical and Electronics Engineering, and Information and Communication Technology.

The up-to-date contributions reported in this book were carefully reviewed by experts and also approved by editors for the last review. All 103 accepted papers were presented and discussed on ICERA 2023, held in Thai Nguyen City, Vietnam, on December 1–2, 2023. The total papers sent to this conference are 232 papers. As a result of the two-stage review process, only 103 excellent contributions were selected for the presentation at the conference and publication in this book. The readers will find here representative samples of the most modern techniques available nowadays for the solution of challenging problems arising in engineering research and application.

We extend our sincere gratitude to the writers for their insightful articles that they contributed to the conference. Also, we sincerely appreciate the reviewers' assessments and suggestions for raising the caliber of the chosen papers. Moreover, we would like to specially thank to our Keynote speakers, Prof. Kai-Uwe Sattler (Ilmenau University of Technology, Germany), Prof. Tuan Le Anh (Ha Noi University of Sciences and Technology, Vietnam), Prof. S.A. Sherif (University of Florida, USA), Prof. Roger A. Sauer (RWTH Aachen University, Germany/Gdansk University of Technology), and Prof. Minh T. Nguyen (Thai Nguyen University of Technology, Vietnam), for their valuable and inspiring contributions to scientists, researchers, and listeners. We also thank to the members of the Organizing Committee of ICERA 2023 for their excellent technical and editorial support.

Last but not least, we would like to deeply thank to Springer Publishers and its Editor staff for helping us in the publication of the proceeding volume of this book.

December 2023

Duy Cuong Nguyen
Do Trung Hai
Ngoc Pi Vu
Banh Tien Long
Horst Puta
Kai-Uwe Sattler

Contents

Experimental Study for Superheated Steam Drying of Apple Slice	1
<i>Thi Thu Hang Tran, Tien Cong Do, Thi Hanh Nguyen, Thi Hang Bui, and Kieu Hiep Le</i>	
High Quality Torque for Five-Phase Open-End Winding Non-sinusoidal PMSM Drives	9
<i>Hai T. Do, Tan D. Vu, Ky N. Nguyen, Eric Semail, and Minh T. Nguyen</i>	
Physico–mechanical Properties and Carrier Mobility of HfS ₂ Monolayer	20
<i>Nguyen Hoang Linh, Nguyen Minh Son, Tran The Quang, To Toan Thang, Vuong Van Thanh, Dinh The Hung, and Do Van Truong</i>	
Hybrid Energy Storage on Electric Vehicles	27
<i>Denis Endachev, Alexey Terenchenko, Kirill Karpukhin, Aleksey Kolbasov, Andrey Povaliaev, Pablo Iturralde, and Nguyen Khac Minh</i>	
Identifying Best Input Elements in PMEDM 90CrSi Steel by MAIRCA Method	36
<i>Dinh Van Thanh, Tran Huu Danh, Bui Thanh Danh, Nguyen Van Chien Thang, Nguyen Van Tung, and Do Thi Tam</i>	
Improvement of Motion Stability for AGV Using Pure-Pursuit Path Tracking Algorithm	44
<i>Khong Minh and Vu Thi Lien</i>	
Influence of Dressing Parameters on Wheel Life in Surface Grinding Hardox 500	52
<i>Dinh Van Thanh, Tran Huu Danh, Vi Le The Anh, Nguyen Van Trang, Le Xuan Hung, Vu Ngoc Pi, and Luu Anh Tung</i>	
Influence of the NdFeB Permanent Magnet on Working Characteristics of LSPMSM	61
<i>Trinh Bien Thuy, Le Anh Tuan, Do Nhu Y, and Ngo Xuan Cuong</i>	
Iterative Learning Control (ILC) for Nonlinear System with Slow Variable Parameter and Noise, Applications for Wastewater Treatment Plant contribution	68
<i>Bach Van Nam, Do Trung Hai, and Nguyen Quang Hung</i>	

Interface Formation Induced by Friction Stir Welded Tool Offset in T-lap Joint of AA7075 and AA5083	78
<i>Hao Dinh Duong, Quan Minh Nguyen, Vu Anh Nguyen Le, Thuyen Van Phi, Vu Van Huynh, Nam Hoai Quach, Xuan-Phuong Dang, and Tra Hung Tran</i>	
Investigate a Folding Mechanism Using Cylinder for Operation	85
<i>Thi-Thanh-Nga Nguyen and Anh-Tuan Dang</i>	
Investigation of the Particle Velocity of the Amorphous Powder	96
<i>Vu Duong and Le Hong Ky</i>	
Investigations on Drilling of Al/CFRP/Ti Stacks Using Micro Grooved Drills	102
<i>S. Samsudeensadham, V. Krishnaraj, and R. Zitoune</i>	
Kinematic Model and Fast-Terminal Sliding Mode for Four-Mecanum-Wheeled Mobile Robot	114
<i>Quoc-Dong Hoang, Le Dinh Nghiem, Le Anh Tuan, Pham Duc An, and Nguyen Thi Gam</i>	
Mathematical Modeling of the Mechanical Tensile Strength of the Thick Carbon Steel Plates Weld with the Narrow Gap and Variable Chamfer Angles	121
<i>Minh Hung Ha, Trong Binh Ngo, Quy Huy Trieu, and Hoang Quan Nguyen</i>	
Multi-objective Optimization for Surface Roughness, Cutting Force, and Material Removal Rate During Turning 4340 Alloy Steel by Using Support Machine Vector and NSGA-III	132
<i>Van-Hai Nguyen, Tien-Thinh Le, Nhu-Tung Nguyen, Van-Phong Le, and Thi-Lien Vu</i>	
Multi-objective Optimization of a Two-Stage Bevel Helical Gearbox to Increase Efficiency and Reduce Gearbox Across Section Area	141
<i>Dinh Van Thanh, Tran Huu Danh, Nguyen Van Binh, Bui Thanh Danh, Hoang Xuan Tu, and Nguyen Van Trang</i>	
Multi-Objective Optimization of a Two-Stage Bevel Helical Gearbox to Increase Efficiency and Reduce Gearbox Height	159
<i>Dinh Van Thanh, Tran Huu Danh, Tran Minh Tan, Nguyen Huu Quang, Bui Thanh Danh, Hoang Xuan Tu, and Le Xuan Hung</i>	

Multi-Objective Optimization of a Two-Stage Helical Gearbox to Increase Efficiency and Reduce Bottom Area	177
<i>Dinh Van Thanh, Tran Huu Danh, Nguyen Van Chien Thang, Bui Thanh Danh, Hoang Xuan Tu, and Nguyen Thi Quoc Dung</i>	
Multi-objective Optimization of a Two-Stage Helical Gearbox to Increase Gearbox Efficiency and Decrease Gearbox Length	195
<i>Dinh Van Thanh, Bui Thanh Danh, Vi Le The Anh, Tran Huu Danh, Hoang Xuan Tu, and Nguyen Manh Cuong</i>	
Multi-objective Optimization of a Two-Stage Helical Gearbox with Second Stage Double Gear Sets to Decrease Gearbox Height and Increase Gearbox Efficiency	212
<i>Dinh Van Thanh, Tran Huu Danh, Nguyen Van Binh, Bui Thanh Danh, Nguyen Anh Tuan, Hoang Xuan Tu, and Bui Thanh Hien</i>	
Multi-objective Optimization of a Two-Stage Helical Gearbox with Second Stage Double Gear Sets to Reduce Gearbox Length and Increase Gearbox Efficiency	229
<i>Dinh Van Thanh, Bui Thanh Danh, Nguyen Van Chien Thang, Tran Huu Danh, Nguyen Van Trang, and Hoang Xuan Tu</i>	
Multi-objective Optimization of Dressing Process in Surface Grinding Hardox 500 to Reduce Surface Roughness and Increase Wheel Life	245
<i>Dinh Van Thanh, Tran Huu Danh, Nguyen Duc Anh, Do Duc Dung, Nguyen Van Me, Nguyen Xuan Cuong, Nguyen Van Trang, and Luu Anh Tung</i>	
Observing and Stabilizing Control for an Eccentric Inverted Pendulum	255
<i>Hao Nguyen Dang and Dinh Gia Thi</i>	
Obtaining High-Strength Aluminum Sheets from Powder by Friction-Assisted Lateral Extrusion	261
<i>Viet Q. Vu, Abhishek Pariyar, Laszlo S. Toth, and Satish V. Kailas</i>	
Optimal Design Using BCMO Algorithm of Fuzzy Controllers for Active Suspension Systems	271
<i>Hai-Le Bui</i>	
Optimal Fuzzy Control of Building Models Under Seismic Excitations	277
<i>Van-Bao Hoang, Hong-Son Nguyen, Van-Tuan Nguyen, Thi-Thoa Mac, Dinh-Ba Bui, and Xuan-Thuan Nguyen</i>	

Optimal Motion Planning Motivated by Differential Flatness and Lyapunov-Based Model Predictive Control for 5-DOF Tower Cranes	283
<i>Thi Hue Luu, Van Chung Nguyen, Tung Lam Nguyen, Danh Huy Nguyen, and Duc Chuyen Tran</i>	
Optimization of Multi-TMD Using BCMO Algorithm for Building Models Subjected to Earthquake	293
<i>Ngoc-An Tran, Van-Binh Bui, and Hai-Le Bui</i>	
Optimization of NURBS Fitting for Non-symmetric Acetabulum Bone Surface with Bending Energy	299
<i>Vu Thi Lien</i>	
Optimization of Minimum Quantity Lubricant Conditions in Hard Turning of 9CrSi Steel - An Application of Taguchi Method	306
<i>Thanh-Dat Phan, Thi-Nguyen Nguyen, The-Vinh Do, and Nguyen-Anh-Vu Le</i>	
Optimization of Parameters Affecting the Hammer Rapping Force to Ensure the Durability of the Discharge Electrode Frame, Dust Removal Acceleration and Durability of the Collecting Electrode Plate in the Electrostatic Precipitator	314
<i>Nguyen Anh Tung, Phan Dang Phong, Hoang Van Got, and Hoang Trung Kien</i>	
Ride Performance Analysis of a Semi-active Hydraulic Engine Mounting System of a Passenger Car	332
<i>Hoang Anh Tan, Pham Van Thoan, Nguyen Dinh Tan, Vu Thi Hien, and Le Van Quynh</i>	
Preliminary Results for Optimal Design of the Horn with Complex Welding Profiles in Ultrasonic Welding	341
<i>Khoa Ngo-Nhu, Chec Nguyen-Van, Bich Ngoc Nguyen-Thi, Ngoc Nguyen-Dinh, and Nguyen-Thi Hue</i>	
Radio Path Circuitry of a Novel Transceiver Module of a Promising VHF Digital AESA	354
<i>I. Yu. Malevich, P. V. Zayats, and Minh T. Nguyen</i>	
Development of AFPID Based Stanley Controller to Control the Steering Wheel Angle of Vehicle on Tire Blowout	361
<i>J. Thiagarajan and T. Muthurmalingam</i>	

Research on Simulation and Optimization of the Self-driving Minibus Frame Design	368
<i>Tien Thanh Do, Anh Son Le, Xuan Nang Ho, and Duy Vinh Nguyen</i>	
Research on Using Non-circular Gears in Designing an Uninterrupted Two-Speed Gearbox for Electric Vehicles	378
<i>Phung Van Thom, Nguyen Thanh Trung, Bui Van Tram, Phung Cong Dzung, and Nguyen Hong Thai</i>	
Research on Simulation of Thermal Stability and Optimization of Drum Brakes on Toyota Innova	390
<i>Vu Hai Quan, Nguyen Anh Ngoc, Nguyen Minh Tien, Le Van Quynh, and To Hoang Hai</i>	
Robust Optimal Tracking Control Using Adaptive Disturbance Observer for Wheeled Mobile Robot	399
<i>Nam D. Nguyen and Nam H. Nguyen</i>	
Using WASPAS Method for Scissors Mechanism Selection	407
<i>Trieu Quy Huy, Dinh Van Thanh, Tran Minh Tan, Tran Huu Danh, Nguyen Thi Thanh Nga, and Nguyen Ngoc Thieu</i>	
Signal Communication Solution in Controlling Building Electrical Equipments Applying BMS Technology	415
<i>Trung Dang Ngoc and Duc Ngo Minh</i>	
Singularity Analysis and Singularity Crossing Control of a Five-Bar Parallel Manipulator	426
<i>Nguyen Quang Hoang and Vu Duc Vuong</i>	
STAR-Reconfigurable Intelligent Surface-Assisted Mobile Edge Computing Network with NOMA and RF Energy Harvesting	439
<i>Van-Truong Truong, Mage Mikhail, Van-Nhan Vo, and Dac-Binh Ha</i>	
Stiffness Prediction of 3D Printed Lattice Designs with Continuous Carbon Fibers Based Polylactic Acid Resin	449
<i>Nguyen Ba Thuan, Van Du Nguyen, Ngo Nhu Khoa, Nguyen Thi Thu Dung, Vu Van Dam, Nguyen Quoc Tuan, Nguyen Dang Viet, Khairul Salleh Basaruddin, and Tien-Dat Hoang</i>	
Study of the Lateral Displacement of the Bus in Crosswind Conditions	458
<i>Minh-Hoang Trinh, Tien-Quyet Do, Duy-Suy Pham, Phuc-Hoa Tran, and Trong-Hoan Nguyen</i>	

Technological Factors Contribute to Enhancing Energy Efficiency
in Manufacturing Enterprises: Evidence from the Technology of Switching
and Restructuring Solar Panel in Viet Nam 465
Nhung Tang Cam, Tuan Do Anh, Kiet Ngo Tuan, and Tung-Nguyen Thanh

The Efficiency of Changing Traditional Vehicle by EVs on Taxi Service:
A Case Study on the Energy Consumption and Emission Levels in Hanoi
City 480
*Le Van Nghia, Le Hue Tai Minh, Dam Hoang Phuc,
Duong Ngoc Khanh, and Bui The Dat*

The Study of Effective Regenerative Brakes on Battery Electric Vehicles 489
*Le Hoang Long, Khong Vu Quang, Pham Huu Nam, Pham Van Thoan,
and Pham Minh Hieu*

The Use of a Combined Power Source Vehicles When Converting
an Internal Combustion Engine to an Alternative Fuel to Reduce Emissions
from Exhaust Gases of Carbon Compounds 497
*Van Dung Nguyen, Andrey Y. Dunin, Thin Quynh Nguyen,
Khac Minh Nguyen, Dinh Thi Luong, and Huy Truong Thai*

Theoretical Study for Apple Slice Drying in Superheated Steam 509
Thi Thu Hang Tran and Kieu Hiep Le

Author Index 517



Experimental Study for Superheated Steam Drying of Apple Slice

Thi Thu Hang Tran¹, Tien Cong Do¹, Thi Hanh Nguyen², Thi Hang Bui³,
and Kieu Hiep Le¹ (✉)

¹ School of Mechanical Engineering,
Hanoi University of Science and Technology, Hanoi, Vietnam
hiep.lekieu@hust.edu.vn

² School of Chemistry and Life Sciences,
Hanoi University of Science and Technology, Hanoi, Vietnam

³ Thermal Refrigeration Engineering,
Hanoi College of Electronics and Refrigeration, Hanoi, Vietnam

Abstract. Superheated steam drying is an advanced drying technology in the food processing field. In this study, experimental studies at different drying conditions of superheated steam drying for apple slice are presented. It is observed that the evaporation is faster at higher temperature and higher gas velocity but the effects of temperature are smoother at fast gas velocity. One empirical model is built based on Page's model; this model enables to calculate the average moisture content versus time. The validation results show that the model yields high calculation so this can be applied to simulate the whole drying system. Product quality is also tested in terms of color change, sugar content and acid content to evaluate the application ability of superheated steam drying. Acid content and sugar content lost maximum at 130 °C and 140 °C, respectively.

Keywords: drying · apple · superheated steam · product quality · drying kinetic

1 Introduction

Drying technology is one of heat treatments that are widely applied in agriculture, especially in the post-harvest preservation field [1]. Due to the huge energy consumption of drying process so the continuous improvement of drying in terms of energy efficient and product quality have been received much attention [2]. Using super - heated steam replaces for air to avoid the oxidation and combustion reaction [2]. Thus, super – heated steam drying is the potential drying method to improve the dried product quality. Superheated steam drying (SSD) has been applied for wide range of product likes paddy, wood, soybean, durian, pork, banana, potato, milk, etc. [3–7].

Drying is also the common method to process apples, in which there are several applied dry methods likes hot air drying, freeze drying, hot air drying combined with puffing drying [2]. While hot air drying (HAD) causes negative effects on the apple slice, other methods are complicated and high energy consumption. To evaluate the application

ability of SSD for apple slice in terms of drying kinetic and quality, the experiment work will be carried out for small drying sample at different drying conditions. The evaporation speed and product appearance are examined then one empirical model is built and validated. Additionally, dried products are also collected to analyze the quality in terms of appearance, acid content and sugar content. The study results will contribute to evaluate the application ability of SSD for apple slice.

2 Experiment Description

2.1 Experiment System

The experiment system is built for studying of drying kinetic of small fruit samples are shown in Fig. 1. The main part is one drying chamber which is insulated to prevent the heat loss. Drying sample is put one a tray containing big holes which allow gas flows on both sides of sample. Evaporation is monitored by the decrease of sample mass which is displayed by the sensitive balance 5. The feed water is pumped from (1) to the evaporator (2) then the dry vapor blows to the heater to be heated up to the setup temperature. This superheated steam flows to dry the sample in the dryer then one part blows to the heater to reheat up to the setup temperature and other part is released to the ambience.

Experiment is conducted for apple slice in range of temperature from 110 °C–150 °C and gas velocity from 3 m/s–6 m/s. In this work, the sample thickness is kept constant. Apple is the Breeze New Zealand kind which is bought from local Vinmart, Hanoi.

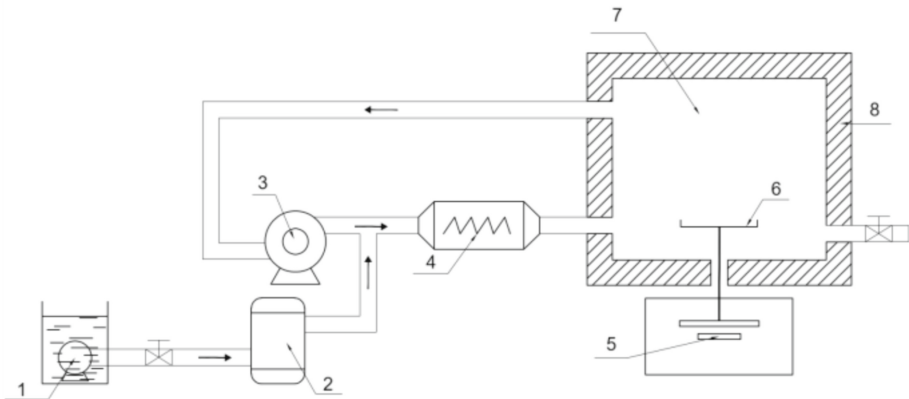


Fig. 1. Diagram of drying system: (1): feed water pump, (2): evaporator, (3): centrifugal fan, (4): electrical heater, (5): balance, (6): sample tray, (7): drying chamber, (8): insulated layer

2.2 Experiment Procedure

Each experiment is conducted for at least three times to make sure the accuracy of data. Experiments are done by seven following:

- Material preparation: Breeze New Zealand apple is chosen from Vinmart, Hanoi. It is cleaned and cut into 2 mm thickness slice.
- Drying system is setup, after drying conditions are reached to the stable status, 1 apple slice is put on the tray.
- Mass of sample is recorded continuously during the drying process until it is almost constant.
- Drying product is collected to analyze the product quality. The total acid content is determined by titration method [8], total sugar and reducing sugar contents are found by Graxianop method.
- Experiment is also conducted parallelly with the drying experiment to predict the initial water content. Several apple slices are checked the mass then they are put into one thermo-plus device for a long time at high temperature to get the solid mass. From the initial mass m_i and solid mass m_s , the initial water content is calculated as:

$$X_i = \frac{m_i - m_s}{m_s} \quad (1)$$

2.3 Data Evaluation

Evaporation

Moisture ratio is a dimensionless function which is expressed as:

$$MR = \frac{X_t - X_e}{X_i - X_e} \quad (2)$$

Where X_i , X_t , X_e are the initial, temporary and equilibrium water contents, kgw/kgs. The equilibrium water content X_e is the final water content of experiment so this is extracted corresponding to the particular experiment. The initial water content X_{in} is 6.7 kgw/kgs.

Color Change

Color change is evaluated based on the lightness, green and red indices of fresh apple and dried apple taken photo by Canon camera. Total difference of dried sample and fresh sample are determined by:

$$\Delta E = \sqrt{(c_{i,r} - c_{ex,r})^2 + (c_{i,g} - c_{ex,g})^2 + (c_{i,w} - c_{ex,w})^2} \quad (3)$$

In which, $c_{i,r}$, $c_{i,g}$, $c_{i,w}$ are red, green, lightness indices of initial samples. $c_{ex,r}$, $c_{ex,g}$, $c_{ex,w}$ are initial red, green, lightness indices of dried samples.

3 Result

3.1 Effect of Drying Conditions on the Evaporation

Changes of moisture rate over time at different temperature and gas velocity are shown in Figs. 2, 3, 4 and 5. For all cases, drying time is about 18–57 min, there are no constant drying period. In one hand, at all gas velocity, evaporation is faster at higher temperature but this effect is significant only at low velocity. In case of 3 m/s, drying time is 30 min at

temperature of 110 °C while this time is about 12 min at temperature of 150 °C. However, at 6 m/s, drying time at 110 °C and 150 °C is 22 min and 11 min respectively. On the other hand, at the same temperature, drying is faster at higher gas velocity. The effect of gas velocity at high temperature is weaker than that at low temperature. These results are because the evaporation is the result of heat and mass transfer between sample surface and bulk vapor. At high temperature results in high temperature difference between sample and bulk gas so the temperature controls this heat and mass transfer. In case of fast velocity, the high gas velocity gives the high heat and mass transfer coefficient so the gas velocity dominates the evaporation in this case.

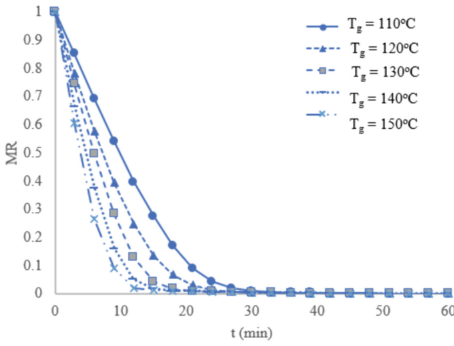


Fig. 2. Evaporation of apple slice at gas velocity of $v_g = 3$ m/s

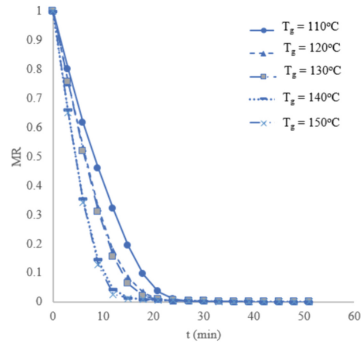


Fig. 3. Evaporation of apple slice at gas velocity of $v_g = 5$ m/s

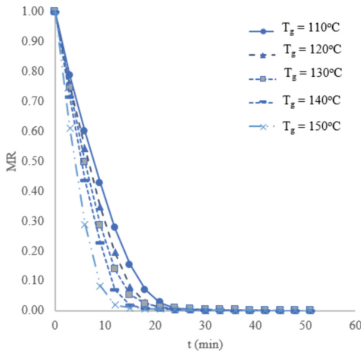


Fig. 4. Evaporation of apple slice at gas velocity of $v_g = 5.5$ m/s

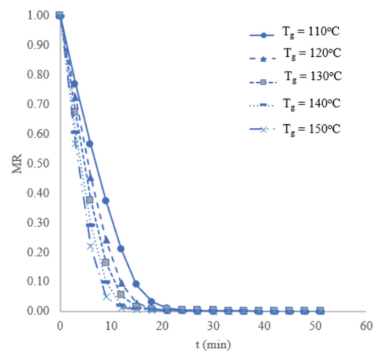


Fig. 5. Evaporation of apple slice at gas velocity of $v_g = 6$ m/s

3.2 Empirical Model

In this section, Page’s model is applied to describe the drying kinetic as [9]:

$$MR = \exp(-kt^n) \tag{4}$$

Where a, b, k, n are parameters determined by fitting MR and experiment data based on square error R^2 . Results show that Page model is the most accurate and the simplest model. The obtained parameters k and n of Page model at individual drying condition are listed as Table 1.

Table 1. Parameters of the empirical model

v_g	T_g	k	n	R^2
3	110	0.02407	1.491	0.9982
3	120	0.04754	1.375	0.9991
3	130	0.05412	1.454	0.9989
3	140	0.09464	1.397	0.9992
3	150	0.1054	1.421	0.9997
5	110	0.03737	1.411	0.9967
5	120	0.0532	1.407	0.999
5	130	0.05141	1.443	0.999
5	140	0.08457	1.422	0.9996
5	150	0.08369	1.452	0.9992
5.5	110	0.04005	1.418	0.9977
5.5	120	0.0493	1.424	0.9984
5.5	130	0.05663	1.423	0.999
5.5	140	0.06092	1.478	0.999
5.5	150	0.09816	1.445	0.9993
6	110	0.0443	1.449	0.998
6	120	0.06186	1.449	0.9992
6	130	0.07855	1.432	0.9993
6	140	0.1034	1.404	0.9996
6	150	0.1098	1.478	0.9998

Comparison of experiment and model is shown in Fig. 6 for selective drying conditions. It is observed that there is much good agreement so the established model is an accurate model and it can be applied for the simulation of the drying system.

3.3 Product Quality

Color Change

Pictures and color change of dried product compared with fresh sample are presented in Table 2 and Fig. 7. It can be observed that at temperature above 130 °C products are burned with the very high color difference. At lower temperatures, the difference

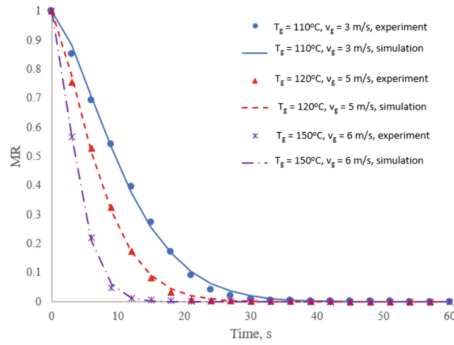








Fig. 6. Comparison of experimental data and simulation

between fresh sample and dried product increases with the increase in temperature but these changes are few. Thus, gas temperature below 130 °C is recommended for drying.

Table 2. Pictures of fresh slice and dried product

Fresh sample	$T_g = 110^\circ\text{C}$	$T_g = 120^\circ\text{C}$
		
$T_g = 130^\circ\text{C}$	$T_g = 140^\circ\text{C}$	$T_g = 150^\circ\text{C}$
		

Marlic Acid Content and Reducing Sugar Content

Mass of marlic acid contained in 100 g basis solid is shown in Table 3. In the superheated steam drying, effects of drying temperature on the marlic acid and reducing sugar contents are significant but not much. The maximum acid content reduction occurs at 130 °C with 30.2% and this content reduces minimum at 110 °C with 18.9%. For the reducing sugar content, the maximum content reduction is at 140 °C with 27.4% and the sugar content decreases at least at 120 °C with 6.7%.

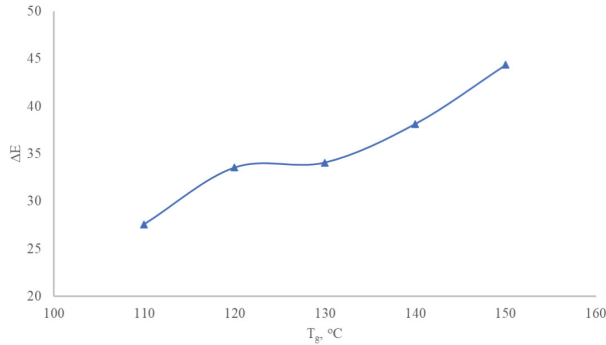


Fig. 7. Color change of product

Table 3. Product quality contents

Gas temperature	Acid content g/100g dried basis	Sugar content g/100 g dried basis
Fresh	2.96	59.41
110 °C	2.43	51.26
120 °C	2.25	55.31
130 °C	2.06	53.17
140 °C	2.39	43.08
150 °C	2.28	50.63

4 Conclusion

Experimental studies of apple slice dried in super-heated steam are presented in terms of evaporation kinetic and product quality. Results show that evaporation speed is faster at higher gas velocity and gas temperature. However, the effect of velocity on the drying kinetic reduces at higher temperature. The empirical model is simple and it gives high accuracy in compared with experiment data. Regarding to product quality, at temperature below 130 °C, color changes not much. Besides, the effects of temperature on the acid

content and sugar contents are not clear. Acid content reduced most at 130 °C while the remained sugar content reaches the minimum value at 140 °C. In next step, the theoretical model should be developed to study the spatial distributions of moisture and temperature inside the sample. The morphology of dried product is also necessary to evaluate in order to find the optimization drying conditions. Besides, the sample thickness is also the important parameter which may prolong the drying time; so, this parameter should be also concerned.






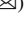
Acknowledgement. This research is funded by the Vietnamese Ministry of Education and Training under grant number B2022-BKA-11.

References

1. Jangam, S.V., Law, C.L., Mujumdar, A.S.: *Drying of Foods, Vegetables and Fruits*, Singapore (2010)
2. Zhu, J., Yuan, Z., Min, C.W.: Effects of different drying methods on the physical properties and sensory characteristics of apple chip snacks. *Lwt Food Sci. Technol.* **154** (2022)
3. Alfy, A., Kiran, B.V., Jeevitha, G.C., Hebbar, H.U., et al.: Recent developments in superheated steam processing of foods-a review. *Crit. Rev. Food Sci. Nutr.* **56**(13), 2191–208 (2016)
4. Le, K.H., Tsotsas, E., Kharaghani, A.: Continuum-scale modeling of superheated steam drying of cellular plant porous media. *Int. J. Heat Mass Transf.* **124**, 1033–1044 (2018)
5. Linke, T., Happe, J., Kohlus, R.: Laboratory-scale superheated steam spray drying of food and dairy products. *Dry. Technol.* **40**(8), 1703–1714 (2021)
6. Patel, S.K., Bade, M.H.: Superheated steam drying and its applicability for various types of the dryer: the state of art. *Dry. Technol.* **39**(3), 284–305 (2020)
7. Lum, A., Mansouri, S., Hapgood, K., Wo, M.W.: Single droplet drying of milk in air and superheated steam: particle formation and wettability. *Dry. Technol.* **36**(15), 1802–1813 (2018)
8. Pierre, D.: Acid-base titration. *Undergrad. J. Math. Model. One Two* **10**(1) (2018)
9. Midilli, A., Kucuk, H., Yapar, Z.: A new model for single-layer drying. *Dry. Technol.* **20**(7), 1503–1513 (2007)



High Quality Torque for Five-Phase Open-End Winding Non-sinusoidal PMSM Drives

Hai T. Do¹ , Tan D. Vu¹ , Ky N. Nguyen² , Eric Semail² ,
and Minh T. Nguyen¹  

¹ Thai Nguyen University of Technology, Thai Nguyen University, Thai Nguyen 240000, Vietnam

nguyentuanminh@tnut.edu.vn

² Univ. Lille, Arts et Metiers Institute of Technology, Central Lille, Junia, ULR 2697 - L2EP, 59000 Lille, France

Abstract. This paper presents a novel control scheme using the well-known field-oriented control (FOC) technique and a simple adaptive linear neuron (Adaline) to obtain smooth torque with a five-phase open-end winding non-sinusoidal permanent magnet synchronous machine (PMSM). For a given supply voltage value, the open-end winding structure results in higher allowable phase voltages, leading to a higher maximum rotating speed. Compared to a sinusoidal back electromotive force (back-EMF), a non-sinusoidal back-EMF leads to lower manufacturing costs and higher torque density. Nevertheless, unexpected current harmonics and torque ripples are consequently generated by the harmonics in back-EMFs, reducing control quality of the electric drive. In this study, the Adaline-FOC-based control scheme is proposed to eliminate the unwanted current harmonics and especially the torque ripples for a high-quality torque machine drive. Numerical results are presented to prove the effectiveness of the proposed scheme.

Keywords: Multiphase machine · non-sinusoidal back-EMF · torque ripple elimination · adaptive linear neuron

1 Introduction

With high functional reliability, multiphase drives have been a suitable choice in many applications such as transportation, submarine, and wind turbines [1]. Compared to the conventional three-phase topology, multiphase one (the number of phases $n > 3$) has more degrees of freedom for machine design and control. Accordingly, several advantages of the multiphase structure can be listed as fault tolerance, low power per phase rating, and smooth torque [2, 3].

The multi-reference-frame theory is a base to analyze an electric machine, especially multiphase ones [4]. For example, a machine with n phases is characterized by $(n - 1)/2$ (n is odd) and $(n - 2)/2$ (n is even) two-dimensional planes (reference frames). One plane is associated with a harmonic group. Ideally, in each plane, there is only one harmonic of back-EMF (or current). In this case, constant torque is perfectly generated

by constant dq currents, facilitating popular proportional-integral (PI) controllers [5]. An increase in n leads to having more reference frames and more harmonics are allowable in back-EMFs. This characteristic cannot be found in a three-phase machine with only one two-dimensional frame, requiring sinusoidal back-EMFs and currents. Therefore, the multiphase topology has fewer constraints on design than a three-phase counterpart.

Nevertheless, the machine manufacturing could unprecedentedly generate more harmonics (> 1 harmonic per frame), conflicting the multi-reference-frame theory. Possible impacts of these unexpected harmonics on current control have been discussed and solved in several recent studies. Indeed, one of the negative impacts is the appearance of unwanted current harmonics appear, resulting in time-variant dq currents. The approach in [6] for a high-speed three-phase machine drive, or in [7, 8] for five- and seven-phase machines could eliminate unwanted current harmonics, improving current control quality. However, in this case, torque pulsation still exists due to the interaction between the desired current harmonics and unwanted back-EMF harmonics.

Maximum torque per ampere (MTPA) in [9] applied for arbitrary waveforms of back-EMFs has been used to theoretically obtain the constant torque. However, varying current references for control in [9] require high bandwidth controllers but not PI controllers such as hysteresis controllers with high switching losses. Study [10] presents another approach but its results and those of [9] are similar. Several control techniques, such as model predictive control [11, 12] or pulse width modulation (PWM) carrier phase shift [13], have been applied to reduce torque ripples. However, torque ripples caused by unexpected back-EMF harmonics cannot be eliminated. Notably, in [14], an Adaline has been applied to eliminate torque ripples caused by unwanted back-EMF harmonics for a seven-phase star-connected winding machine without the use of Adalines for current harmonic eliminations.

In this study, an adaptive control scheme is introduced to derive smooth torque under the existence of plenty of harmonics in back-EMFs. Besides five Adalines used to eliminate unwanted current harmonics as proposed in [6–8], an additional Adaline is used for torque ripple eliminations. The conventional FOC technique and the Adaline are properly combined. Knowledge of machines such as harmonic components is used to optimize the Adaline, avoiding the calculation burden. The proposed Adaline-FOC-based scheme is validated with numerical results on a five-phase open-end winding non-sinusoidal PMSM drive.

This paper is organized as follows. Section 2 presents the mathematical modeling of a five-phase open-end winding PMSM; a solution to eliminate current harmonics is discussed in Sect. 3. Section 4 proposes a control scheme to obtain high quality torque. Finally, Sect. 5 presents numerical results.

2 Modeling of a Five-Phase Open-End Winding PMSM

A five-phase PMSM with non-sinusoidal back-EMF and equally shifted phases in the open-end winding configuration is considered in this study. Hypotheses for the back-EMF are described as follows: 3rd harmonic has the second highest proportion after 1st harmonic; the unwanted harmonics (5th, 7th, 9th, and 15th) have modest proportions.

The schematic diagram of the considered drive is presented in Fig. 1. One DC-bus voltage supplies two inverters VSI_1 and VSI_2 . Notably, each leg in VSI_1 and its

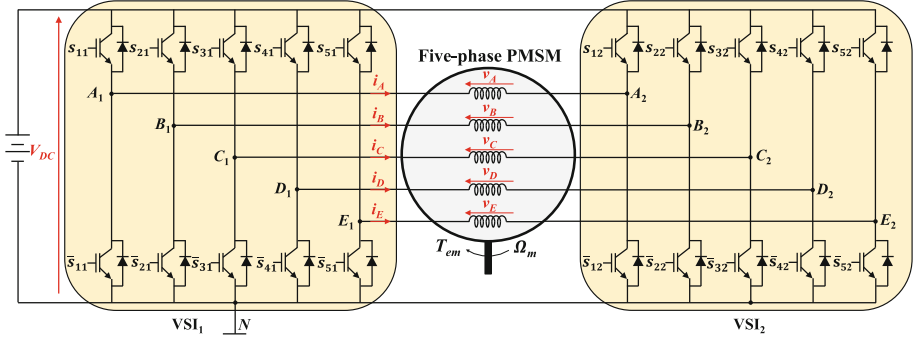


Fig. 1. Schematic diagram of a five-phase open-end winding PMSM supplied by two VSIs.

corresponding leg in VSI₂ are used to feed one phase of the machine, representing the open-end winding structure. The maximum allowable voltage of one machine phase is V_{DC} that is two times higher than the star connection.

In general, the voltages applied to the machine phases can be written as

$$\underline{v} = \begin{bmatrix} v_A & v_B & v_C & v_D & v_E \end{bmatrix}^T = \begin{bmatrix} v_{A_1N} & v_{B_1N} & v_{C_1N} & v_{D_1N} & v_{E_1N} \end{bmatrix}^T - \begin{bmatrix} v_{A_2N} & v_{B_2N} & v_{C_2N} & v_{D_2N} & v_{E_2N} \end{bmatrix}^T \quad (1)$$

where \underline{v} is the 5-dimensional vector referring to five phase voltages of the machine; $(v_{A_1N}, \dots, v_{E_1N})$ and $(v_{A_2N}, \dots, v_{E_2N})$ are leg voltages of VSI₁ and VSI₂ compared to the neutral point N , respectively.

The calculation of phase voltages and electromagnetic torque can be expressed as

$$\underline{v} = R\underline{i} + [L] \frac{d\underline{i}}{dt} + \underline{e} \quad (2)$$

$$T_{em} = \underline{e}^T \underline{i} \quad (3)$$

where \underline{i} and \underline{e} are the 5-dimensional vectors of phase currents and back-EMFs, respectively; R is the resistance of one phase; $[L]$ is a 5 by 5 stator inductance matrix; T_{em} is the electromagnetic torque.

Table 1. Fictitious machines and odd harmonics of a five-phase machine.

Fictitious machine	dq frame	Associated harmonic in natural frame ($m \in \mathbb{N}_0$)
The first machine (FM1)	$d_1 - q_1$	$\underline{1}, \underline{9}, 11, \dots, 5m \pm 1$
The second machine (FM2)	$d_3 - q_3$	$\underline{3}, \underline{7}, 13, \dots, 5m \pm 2$
Zero-sequence machine (ZM)	z	$\underline{5}, \underline{15}, \dots, 5m$

With the FOC technique, Clarke [*Clarke*] and Park [*Park*] matrices [8] are applied to convert parameters of the machine from natural frame into rotating frames (dq frames).

The transformation for phase currents is presented as

$$\begin{bmatrix} i_{d1} & i_{q1} & i_{d3} & i_{q3} & i_z \end{bmatrix}^T = [Park][Clarke] \begin{bmatrix} i_A & i_B & i_C & i_D & i_E \end{bmatrix}^T. \quad (4)$$

In dq frames, the machine can be represented by two fictitious 2-phase machines FM1 (with frame d_1-q_1) and FM2 (with frame d_3-q_3), and one zero-sequence machine ZM (with axis z). Each fictitious machine is associated with a group of harmonics in natural frame as presented in Table 1 [4]. The subscripts “1” and “3” in dq frames (d_1-q_1 and d_3-q_3) refer to the ranks of main harmonics in these frames. Notably, values of machine parameters, such as currents and back-EMFs, are expected to be constant in dq frames to facilitate current control as well as to obtain high quality torque. In other words, there are no harmonics in dq frames.

3 Elimination of Current Harmonics

According to [6–8], the low-frequency current harmonics in dq frames are generated by the unwanted back-EMF harmonics (5^{th} , 7^{th} , 9^{th} , and 15^{th}) and the inverter nonlinearity (dead-time voltages). These current harmonics have frequencies of 10θ (for i_{d1} , i_{q1} , i_{d3} , i_{q3}), 5θ and 15θ (for i_z) in dq frames as described in Table 2 where θ is the electrical position of the machine. Current harmonic amplitudes depend on several parameters such as the harmonic distribution in back-EMF, rotating speed, switching period, inverter dead time, and DC-bus voltage. Due to the complication of the real-time drive systems, these parameters need to be automatically identified in real time to correctly eliminate the current harmonics. Therefore, five Adalines have been proposed in [6] for five dq currents in three frames (d_1-q_1), (d_3-q_3), and z . The combination between the five Adalines and back-EMF harmonics can effectively eliminate current harmonics.

Table 2. Unwanted current harmonics of a non-sinusoidal five-phase machine.

Fictitious machine	dq frame	Current harmonics by unwanted back-EMFs	Current harmonics by dead-time voltages
FM1	d_1-q_1	10θ	10θ
FM2	d_3-q_3	10θ	10θ
ZM	z	$5\theta, 15\theta$	0

From [8], the i_{q1} current control scheme with current harmonic eliminations is described in Fig. 2a with the Adaline for current in Fig. 2b. Current i_{q1} is controlled by a PI controller. An adaptive compensating voltage v_{q1_com} generated by the Adaline and the estimated q_1 -axis back-EMF E_{q1} are used to eliminate a harmonic of 10θ in dq frame. In a five-phase open-end winding machine, there are five dq currents, leading to five Adalines for current harmonic eliminations.

However, the elimination of current harmonics in [6–8] cannot guarantee a constant torque because the interaction between the main harmonics of currents (1^{st} and 3^{rd})

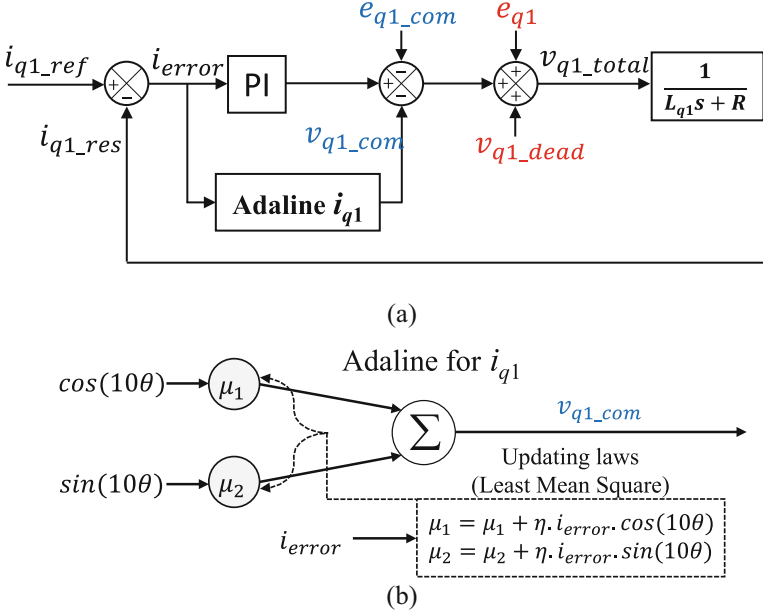


Fig. 2. Current harmonic elimination: (a) Control scheme of one of five dq currents, (b) Adaline structure.

and the unwanted back-EMF harmonics (5^{th} , 7^{th} , 9^{th} , and 15^{th}), causing the torque harmonic of 10θ . Table 3 describes the rank of torque ripples generated by the imposed current harmonics and unwanted back-EMF harmonics. Figure 3 shows the elimination of current harmonics (i_{q1} and phase current i_A from 0.015 s) and the existence of torque ripples with harmonic 10θ (about 18%) even when the current harmonics in dq frames have been eliminated [8].

Table 3. Torque ripples generated by unwanted back-EMF harmonics in fictitious machines.

Fictitious machine	Current harmonics after compensation	Unwanted back-EMF harmonics	Torque harmonics
ZM1	1θ	9θ	10θ
ZM2	3θ	7θ	10θ
ZM	0	$5\theta, 15\theta$	0

4 Eliminations of Torque Ripples

The proposed Adaline-FOC-based control scheme is described in Fig. 4 with the Adaline for torque described in Fig. 5. The purpose of the Adaline for torque in the control scheme is to determine compensating torque T_{emcom} . Then, the compensating currents

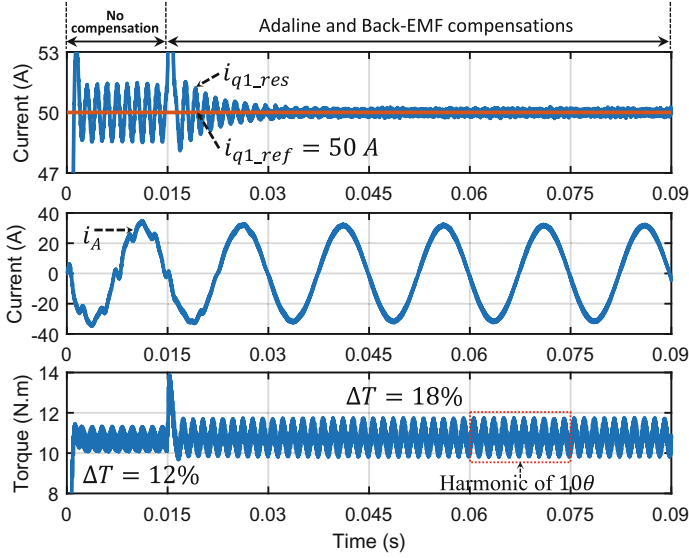


Fig. 3. Elimination of harmonics in i_{q1} , phase-A current, and torque at 60 rad/s.

i_{com} (i_{dqcom}) can be calculated from T_{emcom} by using Maximum Torque Per Ampere (MTPA) [14]. However, only main harmonics (1st and 3rd) of the speed normalized back-EMF are considered to calculate currents, the original MTPA becomes simplified MTPA in this study. Finally, the error between T_{em} and its reference value T_{emref} is minimized. The desired compensating torque can be expressed as

$$T_{emcom}^* = T_{emref} - T_{em} = \mu_0^* + \mu_1^* \cos(10\theta) + \mu_2^* \sin(10\theta) \quad (5)$$

where μ^* is the constant term of the compensating torque; (μ_1^* , μ_2^*) are respectively coefficients representing torque harmonics 10θ . Therefore, the compensating torque T_{emcom}^* is expressed by three coefficients (μ_0^* , μ_1^* , μ_2^*).

The output of the Adaline in Fig. 5 is given by

$$y = \mu_0 + [\mu_1 \cos(10\theta) + \mu_2 \sin(10\theta)] \quad (6)$$

where θ is the electrical position; (μ_0 , μ_1 , μ_2) are three weights corresponding to the three coefficients of the desired compensating torque in (5).

The Adaline weights are updated by Least Mean Square rule [14, 15] at each sampled time k . An example for weight updating with μ_1 is expressed by

$$\mu_1(k+1) = \mu_1(k) + \eta [T_{emref} - T_{em}(k)] \cos(10\theta) = \mu_1(k) + \eta T_{error}(k) \cos(10\theta) \quad (7)$$

where η is the learning rate; T_{error} is the error between reference torque T_{emref} and total torque T_{em} ; T_{em} is derived from phase currents and estimated back-EMFs in ‘‘Torque estimation’’ block in Fig. 4 using (3).

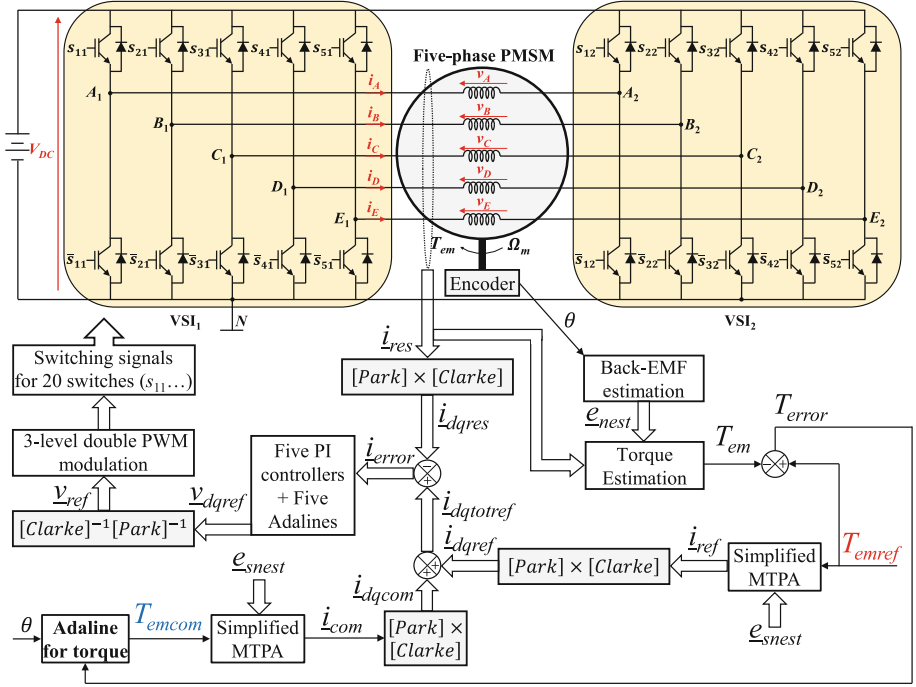


Fig. 4. The proposed Adaline-FOC-based control structure to eliminate torque ripples.

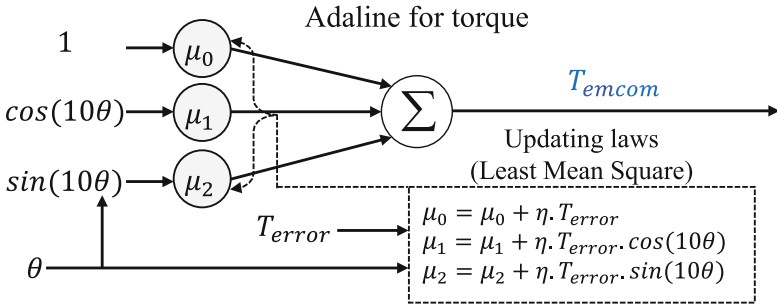


Fig. 5. Adaline structure to eliminate torque ripples.

Learning rate η needs be properly chosen and within $[0, 1]$ to guarantee the system stability. Its value mainly depends on the sample time, amplitudes and phases of harmonics of the learned signal (T_{emcom}). The Adaline weights are updated to converge to the desired coefficients of the compensating torque in (5) as follows

$$\left\langle \mu_0(k) \rightarrow \mu_0^*; \mu_1(k) \rightarrow \mu_1^*; \mu_2(k) \rightarrow \mu_2^* \right\rangle. \quad (8)$$

Finally, the torque ripples are eliminated by the proposed control scheme.

5 Numerical Results

Numerical results to verify the effectiveness of the Adaline-FOC-based scheme (Fig. 4) are obtained with MATLAB Simulink. Parameters of the studied drive are described in Table 4. Two VSIs are controlled with the 3-level double modulation PWM (at 15 kHz). Five dq currents are controlled by five PI controllers and five Adalines for current harmonic eliminations as described in [6].

As previously assumed, six back-EMF harmonics (1st, 3rd, 5th, 7th, 9th, 15th) with the proportions in Fig. 6 are used to model the 5-phase machine. The reference torque T_{emf} of 10 N.m (rated torque) is imposed at 750 r/min to verify the proposed scheme.

Table 4. Electrical parameters of the studied five-phase PMSM drive.

Parameter	Unit	Value
Stator resistance R	m Ω	9.1
Self-inductance L	mH	0.09
Mutual inductance M_1	mH	0.02
Mutual inductance M_2	mH	-0.01
1 st harmonic of speed-normalized back-EMF	V/rad/s	0.1358
Number of pole pairs p		7
Rated torque	N.m	10
DC-bus voltage V_{DC}	V	48
PWM switching frequency	kHz	15
Learning rate of Adaline for torque η		0.00001

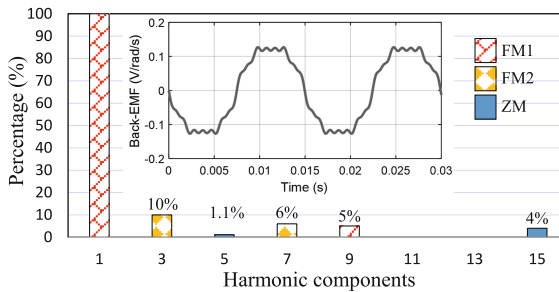


Fig. 6. Speed-normalized back-EMF and harmonic components of the studied five-phase PMSM.

The numerical results are shown in Fig. 7 including the electromagnetic torque, weights of Adaline for torque, dq currents, phase-A current. “No comp.” means that there are no compensations for both unwanted current harmonics and torque ripples. “EMF comp. for current” implies that only estimated back-EMFs are used to eliminate unwanted current harmonics. “EMF+Adalines comp. for current” expresses that both

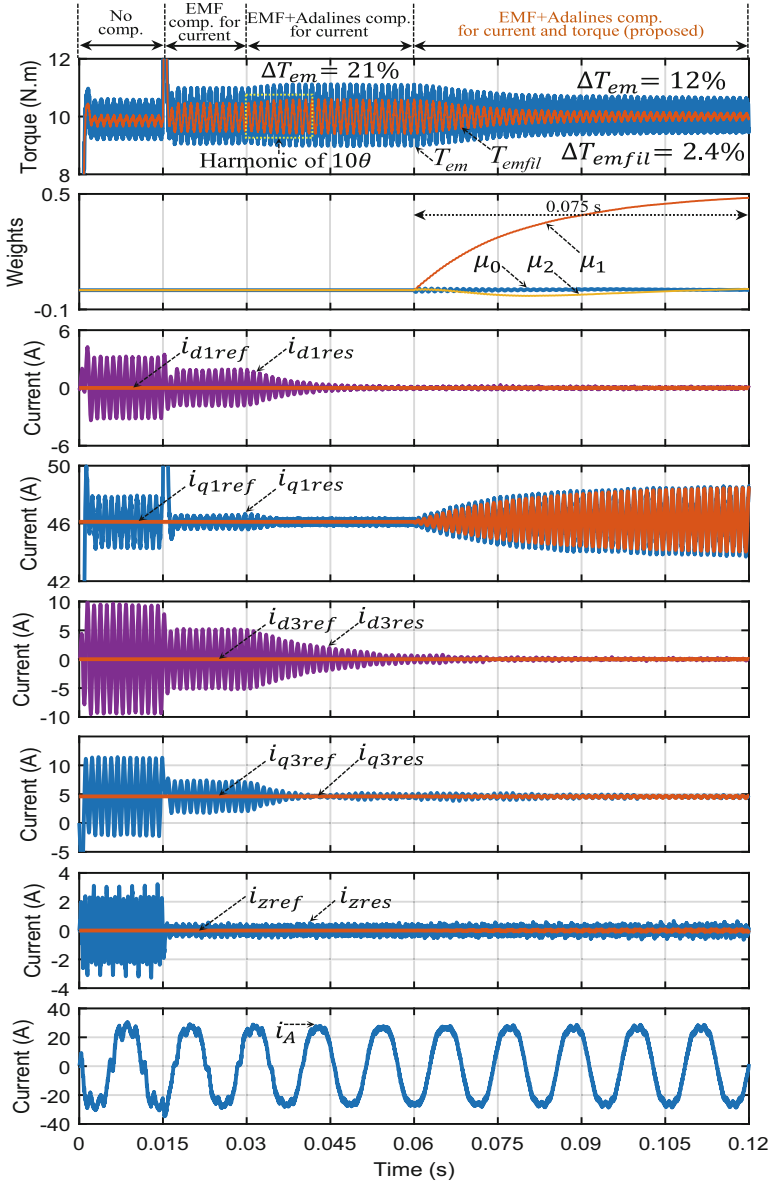


Fig. 7. Numerical results with the electromagnetic torque, weights of Adaline for torque, dq currents, and a phase current at 750 r/min.

estimated back-EMFs and five Adalines are applied to current harmonic eliminations. These first three stages have been discussed in [6]. The last stage presents the addition of the Adaline for torque in the proposed Adaline-FOC-based scheme.

Specifically, the torque ripple can be effectively reduced from 21 to 12% after using the Adaline for torque. The ripple of 12% almost comes from the switching-frequency

zero-sequence components of the open-end winding structure. If the high-frequency components are filtered, the torque ripple is equal to only 2.4%. The convergence time of the Adaline weights is 0.075 s. Compared to the third stage, only the reference value of i_{q1} becomes time-variant to generate constant torque in the last stage. Current of phase A is presented in the bottom of Fig. 7. By using Adalines for unwanted current harmonics from the second stage to the last stage, the phase current waveform becomes smoother without unexpected current harmonics.

6 Conclusions

The Adaline-FOC-based control scheme for five-phase non-sinusoidal back-EMF machine drives has been proposed and validated in this study. Smooth torque has been generated with a low-cost machine having undesired back-EMFs. Only knowledge of torque harmonics enables the Adaline to be optimized, reducing the calculation burden. The combination of Adalines for current and Adaline for torque not only guarantees pure phase currents but also smooth torque. With the simplicity of Adaline, the Adaline-FOC-based scheme can be effectively used in industry.

Acknowledgments. The authors would like to thank Thai Nguyen University of Technology (TNUT), Viet Nam for the support.

References

1. Yepes, A., Lopez, O., Gonzalez Prieto, I., Duran, M.J., Doval-Gandoy, J.: A comprehensive survey on fault tolerance in multiphase AC drives, Part 1: general overview considering multiple fault types. *Machines* (2022)
2. Ala, G., et al.: Stability of microgrids: an application of virtual synchronous generator. In: Nguyen, D.C., Vu, N.P., Long, B.T., Puta, H., Sattler, K.U. (eds) ICERA 2022. LNNS, vol. 602, pp. 873–880. Springer, Cham (2023). https://doi.org/10.1007/978-3-031-22200-9_92
3. Yepes, A., Gonzalez Prieto, I., Lopez, O., Duran, M.J., Doval-Gandoy, J.: A comprehensive survey on fault tolerance in multiphase AC drives, Part 2: phase and switch open-circuit faults. *Machines* (2022)
4. Semail, E., Kestelyn, X., Bouscayrol, A.: Right harmonic spectrum for the back-electromotive force of an n-phase synchronous motor. In: the 39th IEEE Industry Applications Conference, Seattle, WA, USA, vol. 1, pp. 71–78, October 2004
5. Tran, H.T., Tran, D.L.T., Nguyen, V.Q., Do, H.T., Nguyen, M.T.: A novel framework of modelling, control, and simulation for autonomous quadrotor UAVs utilizing Arduino mega. *Wirel. Commun. Mob. Comput.* **2022** (2022)
6. Wang, L., Zhu, Z.Q., Bin, H., Gong, L.M.: Current harmonics suppression strategy for PMSM with non-sinusoidal back-EMF based on adaptive linear neuron method. *IEEE Trans. Ind. Electron.* **67**(11), 9164–9173 (2020)
7. Vu, D.T., Nguyen, N.K., Semail, E., Nguyen, T.T.N.: Current harmonic eliminations for seven-phase non-sinusoidal PMSM drives applying artificial neurons. In: The International Conference on Engineering and Research Application (ICERA), Thai Nguyen, Vietnam, pp. 270–279 (2020)